Bundesamt für Energie
Office fédéral de l'énergie
Ufficio federale dell'energia
Swiss Federal Office of Energy

Research programme on ambient heat, waste heat and cogeneration of the Swiss Federal Office of Energy

Oil migration on single and two stage heat pump systems

Calibration tests and process design
Phase 1

Prepared by
Michele Zehnder (Ph.D.Student) and
Prof. Dr. D.Favrat
Laboratory of Industrial Energetics (LENI)
1015 Lausanne

on behalf of the
Swiss Federal Office of Energy

December 2000 Intermediate Report

Abstract

The subject of this project is to develop a high performance air water heat pump which is able to be introduced in the *retrofit market*. The system requirements of this market are heating temperatures of 65°C, at ambient temperatures descending until -12°C. To provide higher base performance ratings, the choice of the thermodynamic system is a *two stage heat pump with economizer exchanger* (see figure 2.1). This type of heat pump has improved performances over a large range of application. For heat output adjustment it can be switched to different heating modes (single stage and two stage). For the two stage cycle, the lubrification of the compressors is a major aspect to be studied.

A new online measurement method is applied to evaluate the oil quantity which migrates through the cycle. The absorption spectre of the refrigerant - oil mixture is analysed with a Fourier Transform Infrared (FTIR) spectrometer and the oil quantity can be extracted with high precision (see figure 6.3). (The analysis method has still to be refined.) The infrared spectrometers also allow to control the composition of the refrigerant mixture. A single capture of the spectre needs about 30 seconds. The measurements have to be referred to a regularly updated background spectre, which requests to vacuumize and clean the measurement cell.

The oil migration is simultaneously measured with a high precision densitymeter. The output signal allows a real time follow of the oil quantity and the transmitter will give reliable results after calibration over the application range. Any change of the refrigerant composition cannot be captured by the densitymeter. The resulting density shift would therefore not be attributed correctly to the amount of oil.

For the analysis of oil distribution in the whole heat pump, the measurement method to determine the oil level in the compressor crankcase, and the observation of the oil retention in the evaporator are also discussed in this project.

The heat pump design has been made, based on simulations of the thermodynamic cycle and using existing parts in the laboratory, such as the evaporator and the condenser. The design aim is to avoid oil trapping and to ensure oil transport in the vapour lines of the heat pump (see figure 4.1).

This report has been conducted by the Swiss Federal Office of Energy. The author is responsible for the content and the conclusions presented in this report.

Note: Several figures in this report have been updated from its original.

Résumé

Le projet vise à construire une pompe à chaleur capable de pouvoir être utilisée dans le *marché de remplacement de chaudière*. Dans ce contexte elle doit pouvoir fonctionner aux températures jusqu'à 65°C pour l'eau de chauffage et à des températures d'air qui descendent jusqu'à -12°C. Afin de pouvoir fournir une puissance de chauffage plus élevée à la température de base, le cycle de pompe à chaleur choisi est un *cycle biétagé à échangeur économiseur* (voir figure 2.1). Ce type de cycle montre des performances élevées sur un large domaine d'utilisation. Pour un meilleur suivi de la demande en puissance de chauffage, ce type de cycle peut fonctionner en mode monoétagé ainsi qu'en mode biétagé. La lubrification des compresseurs doit être étudiée pour le cas du fonctionnement biétagé.

Une nouvelle méthode de mesure de la quantité d'huile à été adoptée dans ce contexte. Le spectre d'absorption du mélange réfrigérant - huile est analysé par un spectromètre infrarouge par transformation de Fourier. Ce type de mesure permet d'extraire la quantité d'huile transitante à travers la cellule de mesure avec une précision élevée (voir figure 6.3). (La procédure de mesure est toujours en cours d'être optimisée) En même temps la mesure spectroscopique permet d'analyser la composition du réfrigérant utilisé. Une mesure prend cependant env. 30 secondes et le spectromètre nécessite une prise de spectre de référence dans la cellule vidée et nétoyée une fois tout les jours.

Un suivi de l'évolution de la quantité d'huile migrante est cependant fait en parallèle avec un densimètre à haute précision. Une fois soigneusement calibré ce type de mesure permet un suivi sans maintenance ultérieure. Le densimètre seul ne permet cependant pas une mesure précise, car un changement de la compostion du réfrigérant n'est pas détectable et serait attribué à un changement de quantité d'huile.

Les mesures de niveau d'huile dans les enveloppes des compresseurs et la retention d'huile dans l'évaporateur permettront l'analyse globale de la distribution d'huile dans la pompe à chaleur. Ces points sont également discutés dans ce travail.

Le dimensionnement de la pompe à chaleur à été effectué sur la base d'une simulation du cycle thermodynamique et en considérant des éléments existants au laboratoire (tel que l'évaporateur, le condenseur,...). Le design prend en compte d'éviter au mieux les trappes d'huile et les tubes sont dimensionnés tel que le transport d'huile soit assuré (voir figure 4.1).

Cette étude a été accomplie sur mandat de l'Office Fédéral de l'Energie. L'auteur est seul responsable du contenu et des conclusions.

Zusammenfassung

Ziel dieses Projektes ist die Entwicklung einer effizienten Luft/Wasser Wärmepumpe für den *Sanierungsmarkt*. Die daraus bedingten Systembedingungen sind Heizwassertemperaturen von 65°C bei Aussentemperaturen bis –12°C. Um bei diesem Extrempunkt eine genügende Heizleistung erbringen zu können, fällt die Wahl auf einen *zweistufigen Wärmepumpen-Kreisprozess mit Economizer Wärmeübertrager* (siehe Abb. 2.1). Dieser Kreisprozess zeichnet sich in erhöhten Leistungskennzahlen, auf einem breiten Anwendungsbereich aus. Um eine Anpassung der Heizleistung zu ermöglichen, kann der Prozess in verschiedene Heizbetriebsarten umgestellt werden (einstufig, zweistufig). Beim zweistufigen Betrieb ist die korrekte Schmierung der in Serie geschalteten Kompressoren ein noch ungelöstes Problem und wird in diesem Projekt näher untersucht.

Eine neuartige Messmethode zur Bestimmung des im Kreisprozess mitgeführten Ölanteils wird vorgeschlagen und getestet. Diese Methode beinhaltet Messungen von Absorptions-Spektren des Öl-Kältemittelgemisches mittels eines Fourier Transform Infrarot (FTIR) Spektrometers. Daraus kann der Ölanteil mit hoher Präzision bestimmt werden (siehe Abb. 6.3). (Die Messmethode muss noch verbessert werden.) Mit Hilfe des Spektrometers kann auch die Zusammensetzung des Kältemittelgemisches (R407C) jederzeit überprüft werden. Eine Messung dauert ca. 30 Sekunden. Die Messergebnisse werden mit einer Referenzmessung (Background) verglichen, welche regelmässig durchgeführt werden muss. Dabei muss die Messzelle jedesmal vakuumiert und gereinigt werden.

Gleichzeitig kann der Ölanteil mittels eines präzisen Dichte-Messgwertgebers ermittelt werden. Die hohe Zeitauflösung der Messungen ermöglicht eventuelle Schwankungen mitzuverfolgen. Einmal geeicht, funktioniert dieser Messwertgeber mit hoher Zuverlässigkeit und ohne Wartungsarbeiten. Die Messung der Gemischdichte kann hingegen nicht in jedem Fall auf den Ölanteil zurückgeführt werden. Eine Konzentrationsverschiebung des Kältemittels würde dann einen Auswertungsfehler verursachen.

Um eine Bilanzierung der Ölverteilung in der Wärmepumpe zu ermöglichen, ist eine genaue Messung des Ölstandes in den Kompressoren vorgesehen. Die Rückführung des Öls aus dem Verdampfer wird ebenfalls speziell analysiert.

Die Auslegung der Versuchswärmepumpe wurde mittels einer Simulation des thermodynamischen Prozesses durchgeführt. Verschiedene bereits vorhandene Elemente werden in die neue Anlage integriert (Verdampfer, Kondensator,. . .). Das Design ist speziell auf die Bedürfnisse beziehungsweise auf den Öltransport und die Ölmigration angepasst (siehe Abb. 4.1).

Diese Arbeit ist im Auftrag des Bundesamtes für Energie entstanden. Für den Inhalt und die Schlussfolgerungen ist ausschliesslich der Autor dieses Berichtes verantwortlich.

Contents

1. Introduction

The two oil crisis in the 1970s were the first initiators of heat pump selling world wide. In the 1980s the number of new installed units in Europe diminished again because of the reduced oil price and the lack of technical support of the first generation of the products. Since the late 1990s the market share of the heat pump units grows again continuously. The second generation products are more reliable and several political efforts, introducing quality labels for the products, the manufacturers and the contractors, prevent a new breakdown of the selling.

The European heating market requires mainly heating only heat pumps for residential heating. High performance components are available for new buildings with moderate heating water temperatures. Heat pumps being able to replace oil burners are not yet available. The main improvements for this application type to be made are: *Providing base heating power for the very cold period in winter and ensuring high heating water temperature for the radiator type of heat distribution.* Both conditions can be met by implementing a two stage heat pump cycle, which will be studied in this project.

The lubrication system of the compressors has to be reconsidered, for long term functionality of two stage systems. Oil migration will be in this context the most important phenomenon to be studied.

The oil migration is measured by a high precision densitymeter and is coupled to a infrared spectrometer. The online measurement of the oil amount circulating in the refrigerant loop allows to study the mechanisms of oil transport and to follow oil migration in non steady state conditions, e.g. during the defrosting mode.

2. Thermodynamic concept

The choice of the proposed two stage heat pump cycle is based on the experience collected at LENI over several projects until present. It has been shown, that only this type of cycle results in a real improvement of the performances over the whole range of application, see [5]. Other possibilities of enlargement of the application range are represented by the vapour injection compressor type [1], or the subcooling toping cycle [9]. Oil migration problems however concern only the two stage cycle and will be studied hereafter. The migration phenomenon is analysed and modelled for one stage and two stage configuration of an experimental heat pump unit.

The heat pump cycle is represented by the schema in figure 2.1.

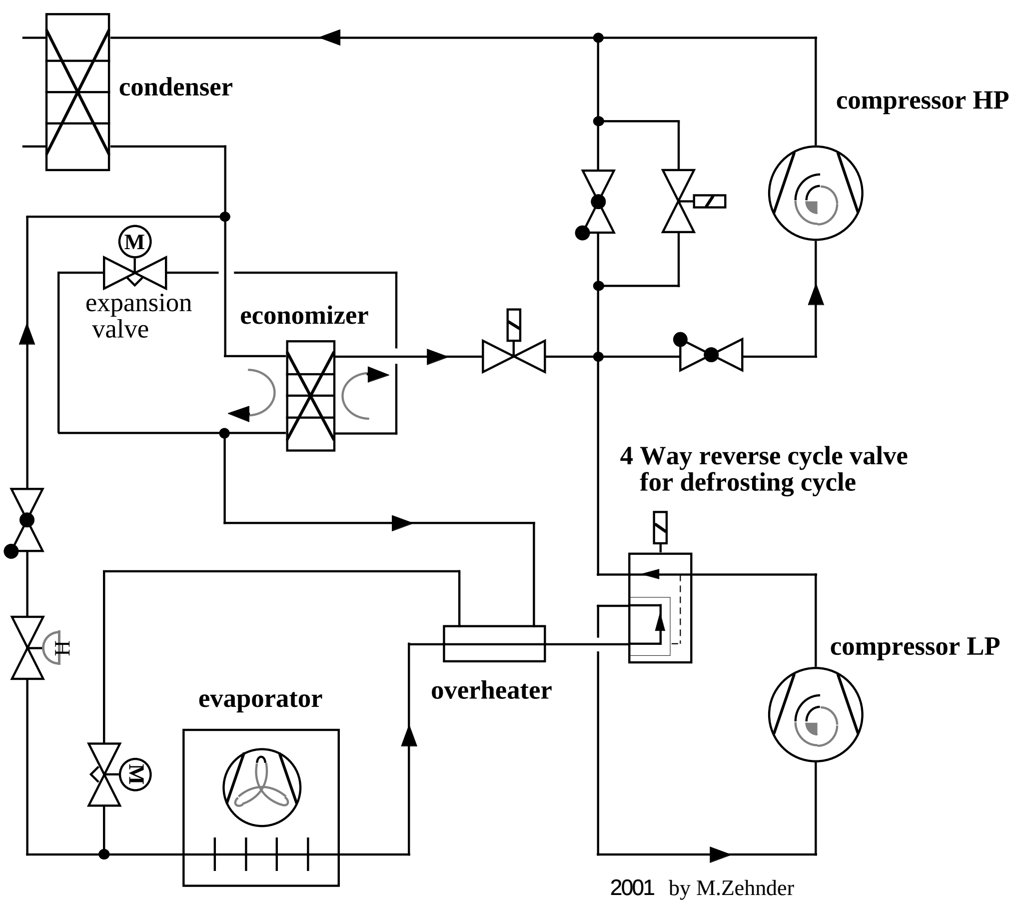

Figure 2.1: *Schematic representation of the two stage heat pump cycle*

All the possible test configurations of the heat pump are shown in the following figures. Pressure levels are represented in different colours, dashed lines represent the part of non circulating fluid.

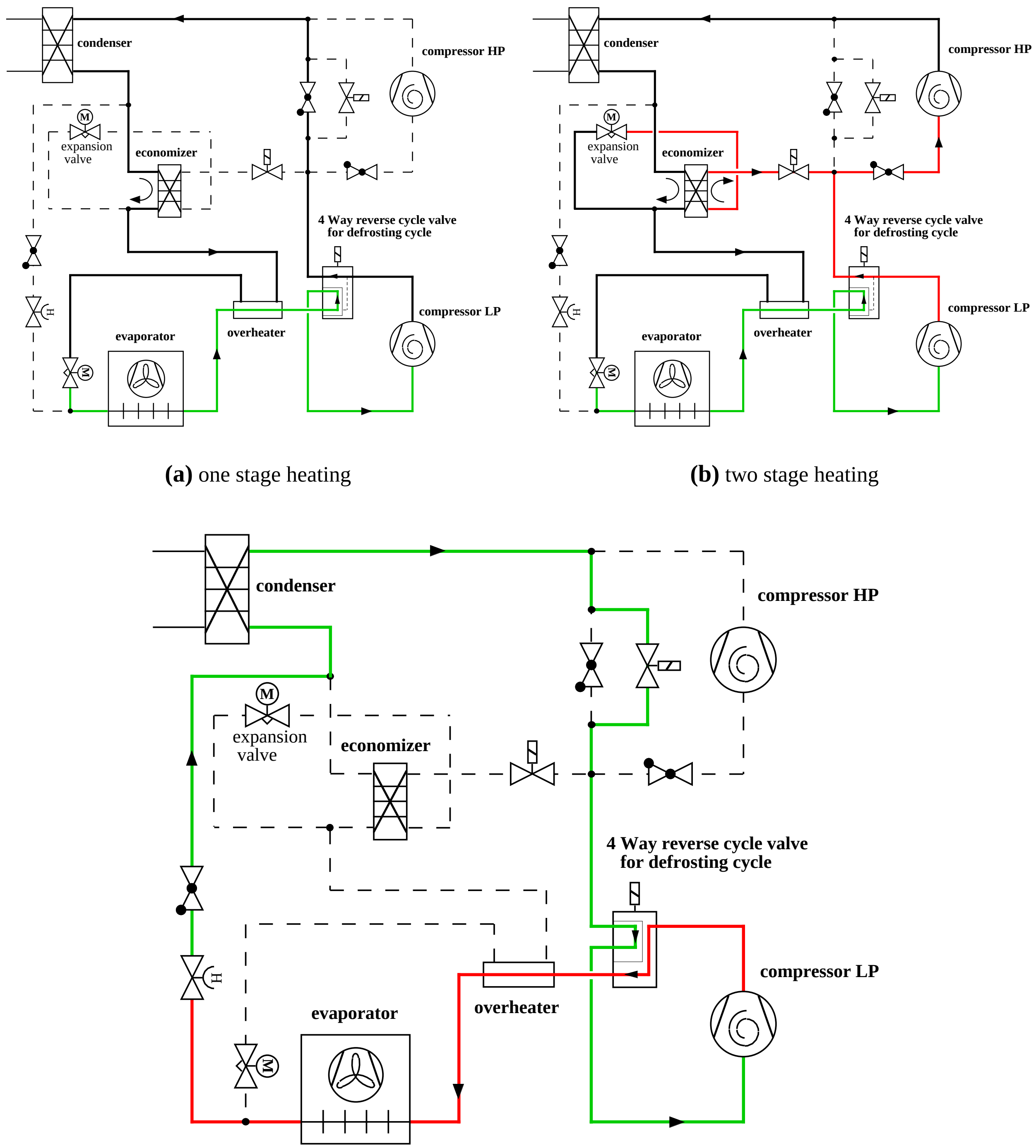

(a) one stage heating

(b) two stage heating

(c) defrosting

Figure 2.2: *Heating modes and defrosting*

2.1 One stage heating mode

Bypassing the HP compressor, the hot gas at the outlet of the compressor is directly injected into the condenser. The condensed refrigerant flows through the economizer without any heat exchange and passes through the suction line overheater. The two phase flow is evaporated and then overheated before entering the compressor. Due to the high discharge temperature, the operational domain is limited.

2.2 Two stage heating mode

Using the two stage configuration with the economizer, the maximum system temperature is lowered and can be controlled by the injected flow amount. After the condenser the refrigerant is subcooled in the economizer before being divided. The minor flow is expanded to the midstage pressure and reenters into the economizer. Fully or partially evaporated it will be remixed with the hot gas from the LP compressor and then enters into the HP compressor. The main refrigerant stream flows through the overheater exchanger. After the main expansion valve it will be evaporated before rejoining the first stage compressor.

2.3 Defrosting mode

The defrosting of the evaporator is initiated by the reverse cycle valve. The hot gas of the LP compressor outlet is directly injected into the evaporator in the inverse sense. The condensed refrigerant is circulating through a bypass line with a manual expansion valve. In the condenser the refrigerant is heated up and evaporated by the heating water, using the thermic inertia of the heating water.

3. Simulation

3.1 Thermodynamic cycle

The simulation of the thermodynamic behaviour of the heat pump is based on the considerations made on earlier projects of this topics (see [8]).

The two stage heating mode is represented on the log P - h diagram in figure 3.1.

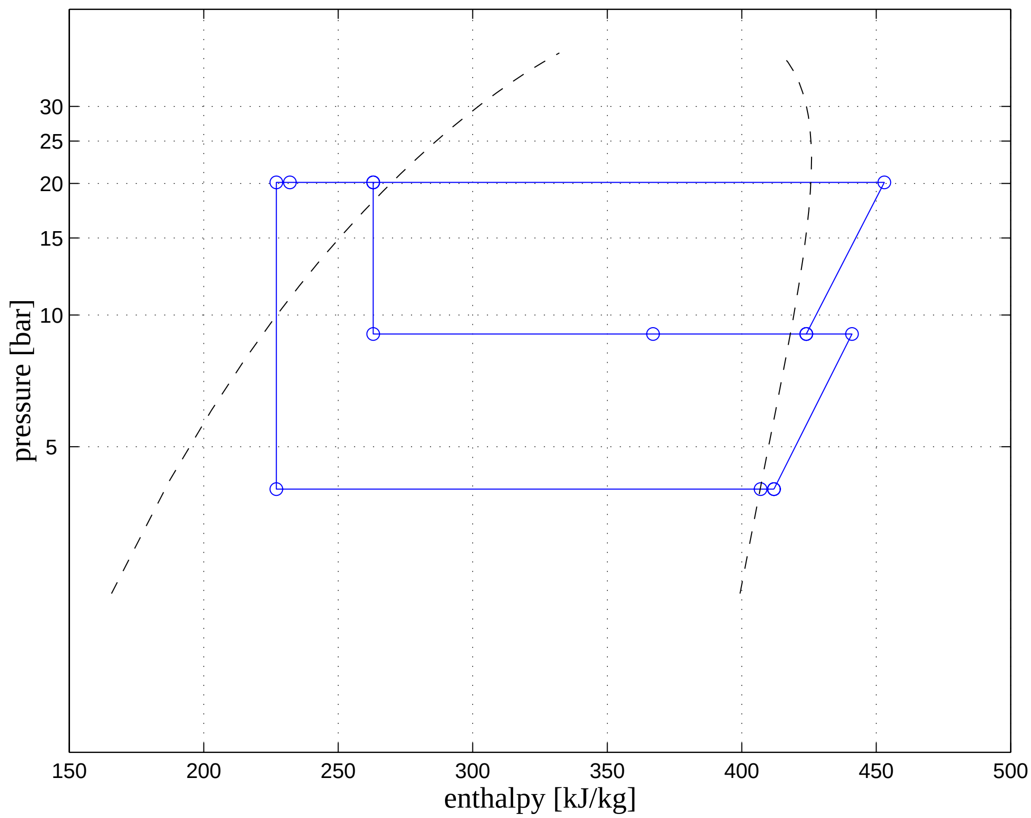

Figure 3.1: *Thermodynamic cycle*

This diagram is issue from a simulation of the heat pump in heating mode at air inlet temperature at 0°C and heating water outlet at 50°C.

3.2 Performance prediction

For the application range which corresponds to an retrofit heating case (heat distribution on radiators and air source heat pump) the simulated COP for the two stage mode is

COP heating = 2.61	eta II,th = 56%
Heat output = 9328 [W]	PR1 = 2.81
El. input = 3575 [W]	PR2 = 3.56
Tmax = 91.79 [°C]	Pcond = 25.31 [bar]
massflow 1 = 31.3 [g/s]	massflow inj = 18.0 [g/s]

Table 3.1: *Performance values at A-12 / W60*

COP heating = 3.75	eta II,th = 58%
Heat output = 11886 [W]	PR1 = 2.26
El. input = 3167 [W]	PR2 = 2.22
Tmax = 71.14 [°C]	Pcond = 20.11 [bar]
massflow 1 = 48.5 [g/s]	massflow inj = 14.3 [g/s]

Table 3.2: *Performance values at A0 / W50*

The indicated performance does not include any auxiliary power (ventilator, solenoid valves, water pump). The experimental COP is expected to be about 10% - 25% lower than the ideal simulated value when both, auxiliaries and defrosting have to be included.

4. System design

4.1 Refrigerant and oil

Refrigerant used is *R407C* (R32 / R125 / R134a [0.23/0.25/0.52 by w.]) Lubricating oil is *EAL Arctic 22 CC* (polyolester especially for Copeland produced and delivered with Copeland compressors). The refrigerant and oil amount will be determined when the physical test rig is constructed.

4.2 Components

The oil migration test utility is composed by the following principal components:

- *compressor LP*: Copeland Scroll ZR 49, 3-phase

  The nominal suction volume rate at 50 Hz is 11.7 m^3/h. Optimum performance is reached at low volume ratios (VR ≅ 2.5).

- *compressor HP*: Copeland Scroll ZR28, monophase

  The high stage compressor is of the same type, but with lower nominal suction volume (6.83 m^3/h).

- *condenser*: Alfa Laval CB50-30H

  This is a brazed plate condenser with heating water in counterflow configuration. Total heat exchange area is 1.5 m^2.

- *economizer*: Swep B8x10 HP

  The economizer is a brazed plate heat exchanger with an exchange surface of 0.184 m^2. After being expanded to the midstage pressure level, the injection flow is partially evaporated and then remixed with the hot gas at the outlet of the LP compressor.

- *expansion valves*: Egelhof RTC 1.0 and RTC 0.5

  For the research project two electronic expansion valves are implemented to regulate independently the mass flow on both stages.

- *evaporator*: Alfa Laval - Artec 2510E32TR6R800A

  The evaporator is an finned tube air evaporator with 24 circuits and 8 passes. The fin pitch is 3.6 mm. The frontal surface of the air circuit is 0.8x0.8 m^2. The total exchange surface on the refrigerant side is 4.58 m^2. The tubes are enhanced surface copper tubes with an internal diameter of 9.5 mm and the fins are of aluminium with a thickness of 0.2 mm.

- *suction line overheater*: Packless HXR 75

  The suction line overheater is integrated for optimizing the evaporator filling and to avoid evaporation pressure drop due to the temperature glide of the refrigerant mixture. The requested overheat in the compressor is reached in the overheater and liquid flashes are avoided to enter the compressor. It is a concentric countercurrent heat exchanger with an internal exchange surface (on the gaseous side) of 0.0175 m^2.

- *reversing cycle valve*: Ranco V6-2103

  This valve enables a reversed cycle defrosting. Only the LP compressor is used for the defrosting period. A hand regulated piston valve is situated on the defrosting bypass line after the evaporator.

4.3 Heat pump layout

The planned two stage heat pump has been developped virtually on a 3D design program. This has been done to optimise volume, pressure drops and to build a compact unit.

The front view from the heat pump unit without the oil distribution lines and the measurement devices is represented in the figure 4.1.

A detailed list of the components and a cost overview is given in the appendix.

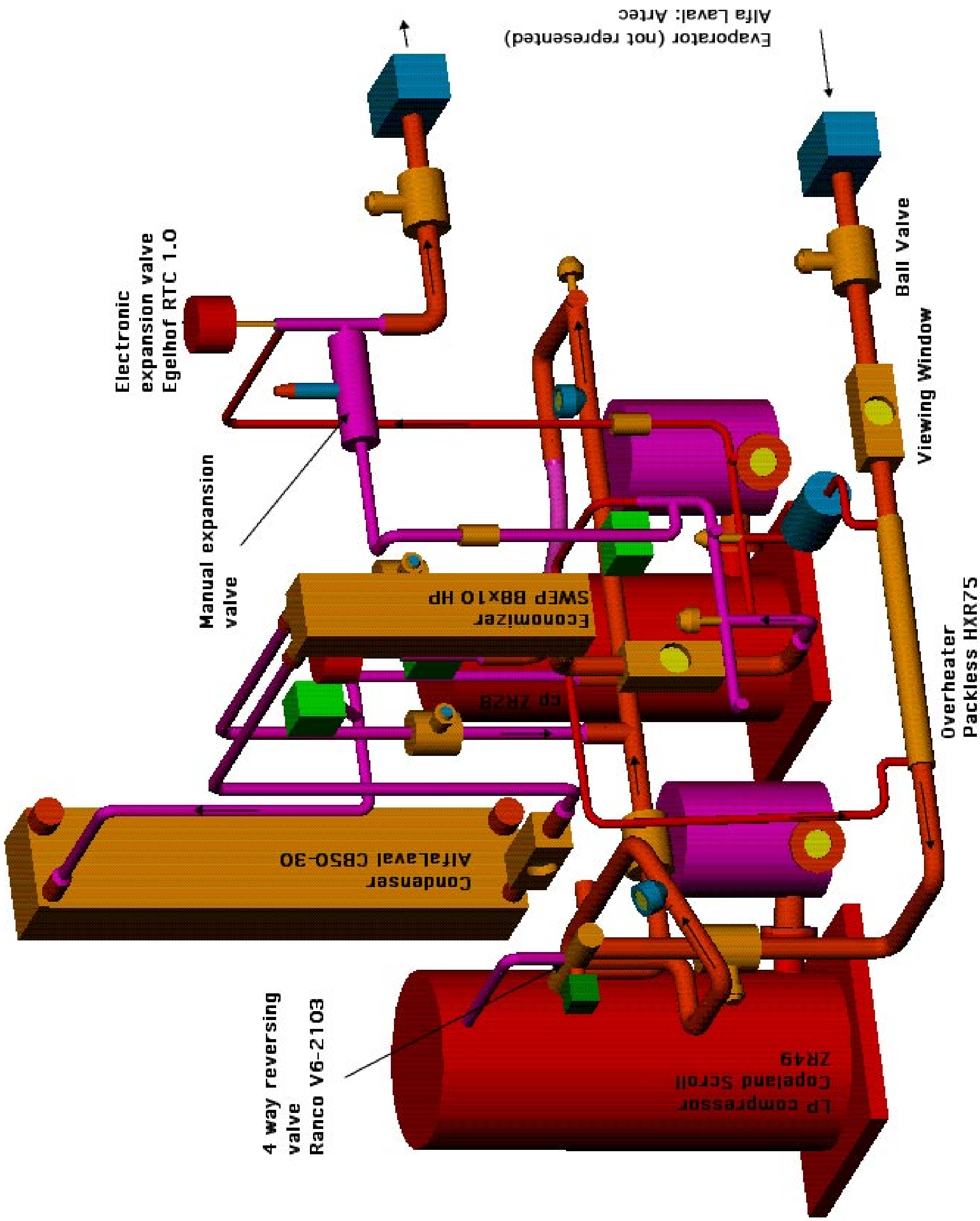

Figure 4.1: *Heat pump layout frontside*

5. Measurement methods

All the measurement points of this unit are represented in the schematic representation of the heat pump unit in figure 5.1.

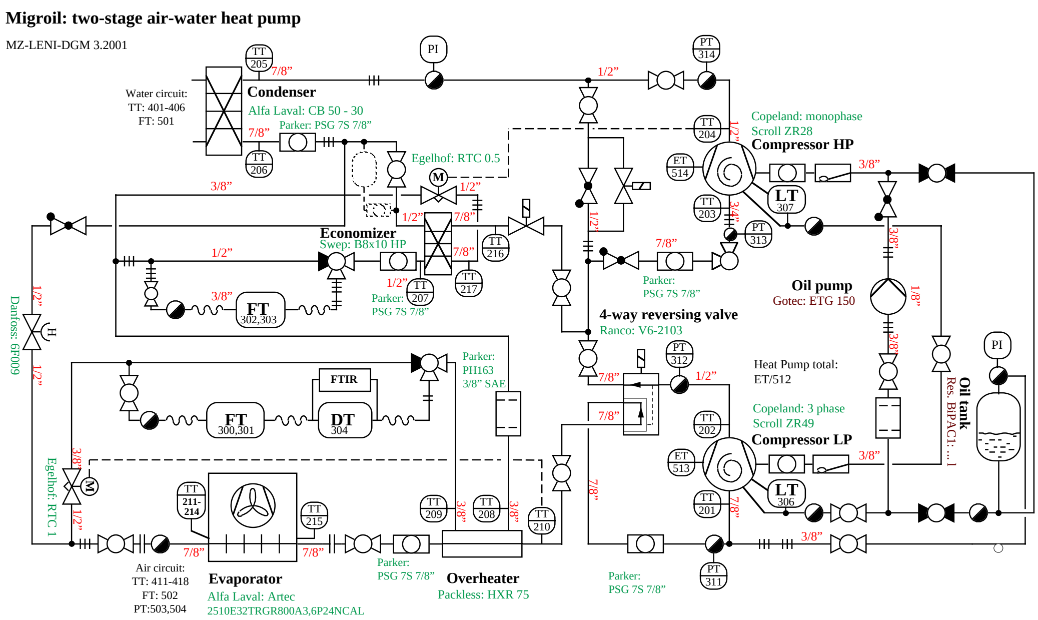

Figure 5.1: *two stage heat pump cycle*

To measure the oil migration at high precision, a densitymeter will be coupled to an Fourier Transform Infrared Spectrometer. By a calibration loop the measurement devices are compared.

5.1 Densitymeter: Bopp&Reuther DIMF 2.0 TRV

The densitymeter is a high precision transmitter with the following indicated performance:

Reproducible measurement precision: $< \pm$ 0.02 % ($\pm$ 0.2 kg/m^3)

For the mean running point refrigerant at 40°C and at 10 K subcooling the relative densities are:

rho R407C = 1073.0 kg/m^3
rho oil POE = 980 kg/m^3

Mixing 2 homogenuos substances (in this example w_{oil} of oil is mixed with $(1 - w_{oil})$ of refrigerant), the specific volume ν of the mixture is given by:

$$\nu^0_{mix} = w_{oil}\, \nu_{oil} + (1 - w_{oil})\, \nu_{refr} \tag{5.1}$$

The density of an *ideal mixture* can be therefore be written as:

$$\rho^0_{mix} = \frac{1}{\frac{w_{oil}}{\rho_{oil}} + \frac{1-w_{oil}}{\rho_{refr}}} \tag{5.2}$$

The effectif mixture volume can diverge from the ideal value and the difference between the real value and the theoretical one can be evaluated by the calibration of the densitymeter.

$$\nu^E = \nu_{mix} - \nu^0_{mix} = f(T, p) \tag{5.3}$$

By the measurement of the mixture density ρ_{mix} the oil weight can be calculated with

$$w_{oil} = \frac{\frac{1}{\rho_{mix}} - \nu^E - \frac{1}{\rho_{refr}}}{\frac{1}{\rho_{oil}} - \frac{1}{\rho_{refr}}} \tag{5.4}$$

Supposing that the density of the pure components and the excess volume are perfectly known for the examined domain, the incertitude of the measurement of the mixture density by the densitymeter is traduced in the value of the oil weight as follows:

$$d(w_{oil}) = \frac{\rho_{refr}\, \rho_{oil}}{\rho_{refr} - \rho_{oil}} \frac{1}{\rho^2_{mix}} d(\rho_{mix}) \tag{5.5}$$

With a measurement precision of the densitymeter of $\pm$ 0.2 kg/m^3 the *absolute precision of the oil weight prediction is about $\pm$ 0.2 %*.

Errors in the correlations used for the pure components ar not taken in account. For this application the error on the refrigerant density is directly traduced into the incertitude of the oil weight dissolved in the refrigerant.

Shifts in the refrigerant composition will greatly influence the incertitude and therefore a online control of the composition has to be included into the study.

5.2 FTIR: Nicolet Magna-IR 560

The Fourier Transform Infrared (FTIR) spectroscopy allows to make online measurements on the refrigerant composition and of the oil weight dissolved in the liquid refrigerant. Measurements can be taken every 30 seconds. The measuring cell is composed by a ATR single reflection diamond, covered by a cylindrical volume. The light source of the spectrometer is liquid nitrogen cooled and the envelop of the spectrometer is purged with cleaned and pressurized air flow (flow rate about 700 l/h, to be improved).

The spectra of the pure oil and the refrigerant were measured to determine the main absorption peaks. (See graphs in the Annex of this report)

EAL Arctic 22 CC: 1020, 1120, *1150*,1220, 1370, 1470, *1740*, 2850, 2920, 2950 cm^{-1}
R407C : 660, *960*, *1060*, *1180*, *1300* cm^{-1}

The interpretation of the different vibrational modes represented by the absorption peaks is not easy and requires good experience in the domain. The author is reffering on several publications where additional information can be found, see [4], [6] and [2]. Web databases are very helpful as well for the main informations, [7]. The superposition of the two fluids shows a free peak at 1740 cm^{-1} for the oil spectre and the precision of measurement for the oil mass fraction is evaluated at 0.1 - 0.2 %. See calibration test results for further informations.

The composition of the R407C refrigerant has to be analysed by deconvolution of the absorption stectrum into its components parts. The calibration tests have to be performed for several couples of temperature and pressure, representing the running conditions in the heat pump cycle.

This additional measurement device allows to make precise analysis on the composition of the refrigerant, which will be the fundament for a precise analysis of the measures with the densitymeter. Using a ternary refrigerant mixture like R407C, a composition control is requested. Additional costs occured in buying a ATR reflexion cell, as the FTIR spectrometer is already property of the laboratory.

5.3 Level detection: Visual level caption on a bypass tube

To know how much oil is accumulated in the compressor shaft, the oil level has to be measured with high precision. A transmitter will be used separately for each compressor.

Different measurement techniques were considered for level detection. After analysis of the test conditions (namely low ratio of the dielectric constant between the gas phase and the liquid), the capacitif and the radar measurement techniques have been rejected. (A radar transmitter has been tested with a precision of $\pm$ 5 mm). The only reliable technique with expected measurement precision of $\pm$ 1 mm is the capture of the level by a camera and the picture can be treated with software (online).

5.4 Flow transmitter: Coriolis K-Flow

The mass flow is measured by two coriolis transmitter. The mass flow is measured very precisely by phase detectors mounted on the vibrating metering tubes. The massflow ranges for the two available models in the laboratory are K20: 0 - 9 kg/min and K100: 0 - 45 kg/min. The operating conditions are T (-95°C/ 180°C) and p (150 bar /limiting pressure by flanges 25 or 40 bar). The cross section of the vibrational tube is K20: 0.174 cm^2 and K100: 0.9423 cm^2.

Zero stability Z is done at K20: 0.0018 kg/min and K100: 0.009 kg/min. The accuracy of the mass flow rate can be calculated with the formula 5.6. (Use common units!)

$$\Delta\dot{M} = (\frac{\dot{M}}{Z} + 0.002) * 100 \tag{5.6}$$

A density signal at an accuracy of $\pm$ 0.003 g/cm^3 (=3 kg/m^3) is also available on the output of the mass flowmeter. The analog output singals are 4 -20 mA. Response time is about 50 ms and therefore negligible for this type of application.

5.5 Oil retention in Evaporator: Separating loop and balance

The oil retention in the evaporator will be determined by separating the refrigerant from the oil with a special loop by washing the evaporator with liquid refigerant. This procedure can only be performed after a sequence of running time. This measurement will complete the analysis by locating possible oil retention in the refrigerant circuit. Improved techniques to analyse oil return to the first stage compressor as well as additional temperature sensors for the local analysis of the heat transfer coefficient will be considered later in this project. The obtained results will be integrated into an advanced simulation of the evaporator according to the heat transfer model developped at the LENI by [10].

6. Calibration loop for oil migration

For calibrating the densitymeter and the infrared spectrometer a test loop has been built before implementing the sensors in the heat pump system. Pure refrigerant (R134a and R407C) is first tested before adding oil. Controling temperature and pressure independently the two sensors will be running at similar conditions like in the heat pump.

The setup of the calibration circuit is represented in figure 6.1.

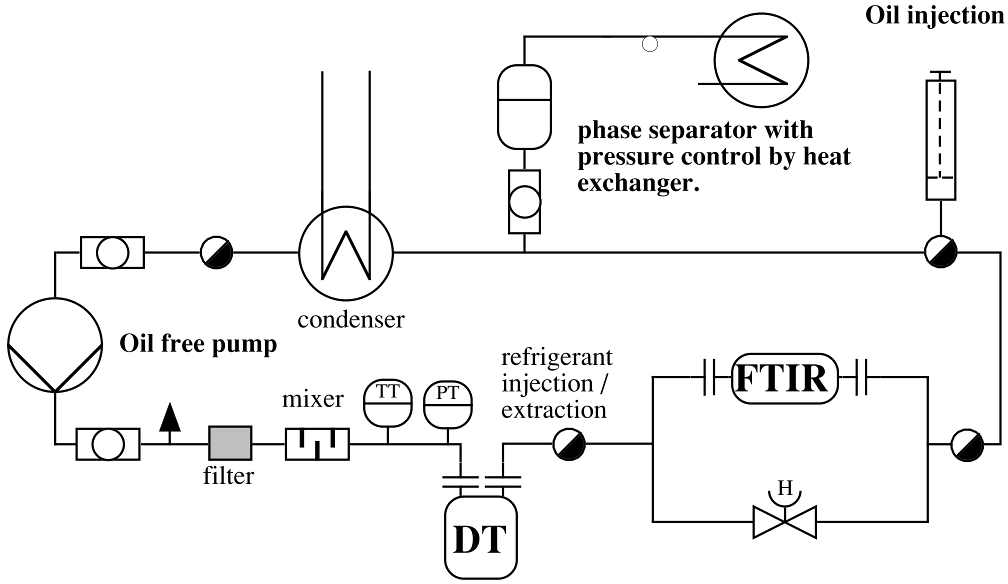

Figure 6.1: *Thermodynamic cycle*

The Volume to be filled by liquid refrigerant was determined to 3.77 l.
This results on a injected refrigerant mass of 4.6 kg for R134a and 4.4 kg for R407C at saturated conditions and at 20°C.

Measurements with pure refrigerant were conducted at the conditions. indicated in table 6.1 and 6.2.

The measured points with R134a show the precision of the densitymeter to the calculated densities (with Refprop 6.01 [3]. For this refrigerant the measured densities are very close to the calculated values. Each temperature point was driven twice to evaluate the repeatability of the measurement. The precision of the repeatable point is at $< \pm$ 0.04 %.

For the measurements with R407C the precision of the calculated value is not so reliable. For the given composition default interaction parameters are used and therefore a less precise evaluation of the density is expected. This is shown by table 6.2.

Series 1: Pure R134a, Densitymeter					
P	T	subcool	rho calc	rho meas	rel error
[bar]	[°C]	[K]	[kg/m3]	[kg/m3]	[%]
11.80	44.80	0.9	1126.2	1126.9	0.06
10.53	39.20	2.1	1150.6	1150.9	0.03
9.79	34.10	4.5	1172.0	1172.1	0.01
9.29	29.90	6.8	1188.9	1188.7	-0.02
8.60	25.00	8.9	1207.9	1207.3	-0.05
8.00	20.10	11.2	1226.2	1225.7	-0.04
6.40	20.10	3.6	1225.3	1225.7	0.03
6.80	25.00	0.7	1206.8	1207.2	0.03
7.91	30.10	0.8	1187.2	1187.4	0.02
9.16	35.40	0.8	1166.0	1166.7	0.06
10.30	39.80	0.7	1147.7	1148.8	0.09
11.75	44.80	0.7	1126.1	1127.4	0.11

Table 6.1: *Calibration points with pure R134a*

Series 2: Pure R407C, Densitymeter					
P	T	subcool	rho calc	rho meas	rel error
[bar]	[°C]	[K]	[kg/m3]	[kg/m3]	[%]
10.30	11.70	8.1	1193.7	1199.3	0.47
11.53	20.70	3.2	1156.7	1162.8	0.53
13.83	30.30	0.5	1114.3	1121.0	0.60
15.55	35.10	0.3	1091.9	1099.4	0.69
17.44	39.90	0.1	1068.3	1076.6	0.77
19.50	44.50	0.1	1044.6	1052.8	0.79
22.12	50.00	0.0	1014.1	1023.6	0.94
19.46	44.50	0.0	1044.5	1052.5	0.76
17.48	40.00	0.1	1067.8	1075.6	0.73
15.57	35.00	0.4	1092.4	1099.2	0.62
13.70	30.00	0.4	1115.6	1122.2	0.59

Table 6.2: *Calibration points with pure R407C*

Two series of oil concentration measurement (with oil EAL Arctic 22 CC) were conducted on the calibration loop. First R407C was measured at the nominal oil concentration of $0 - 8.91\%$.

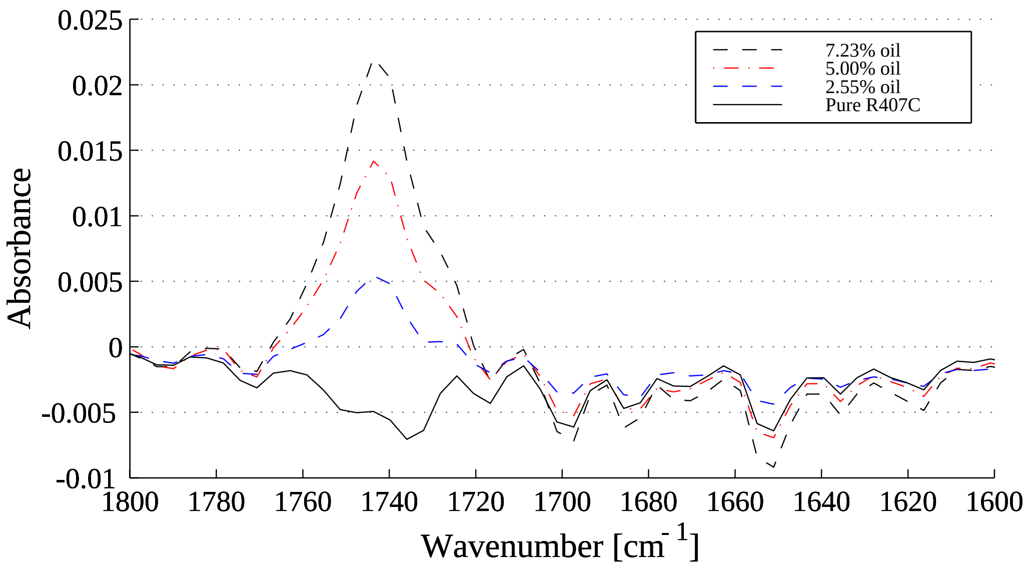

Figure 6.2: *Visualisation of EAL Arctic 22 CC oil peak for a FTIR spectrum*

Taking the underlaying surface of the peak allows to make a quantification of the oil concentration. In figure 6.2 the free oil peak is shown clearly. However the baseline still contains traces of H_2O whose absorbance spectrum is within 1200 - 2000 and 3500 - 4000 cm^{-1}. The purging technique of the spectrometer has to be analysed and improved to eliminate all residuals of CO_2 and H_2O in the background spectre.

This first test run with different oil concentration was made in order to evaluate the sensitivity of oil concentration which could be obtained by such a technique. The regression including all measurement point is shown in figure 6.3. Similar results were obtained with R134a and oil mixture, but only the nominal concentrations of 0% , 0.45% and 0.9% were examinated. Repeatability of these results could not reached in order to predict actual oil concentration at high precision. The measurement method is still in progress and highly reliable results are still expected.

Oil quantification with the densitymeter did not show the expected accuracy. The measured mixture density resulted in a underpredicion of the oil concentration by a factor 3 !! (see figure 6.4) for the mixture oil-R407C mixture and by a factor 1.4 with oil-R134a. Equation 5.4 was used to calculate oil concentration. The oil was assumed to be a non compressible fluid with a density of 987 kg/m^3 at 20°C.

In order to control the oil migration through the densitymeter, the concentration was examinated by an independant verification method. The method consisted to remove a determined mass of mixture from the suction line of the densitymeter into a recipient. The mass remaining after gentle evaporation of the refrigerant over 12 hours represents pure oil. By this method, the same oil concentration as the nominal value was measured.

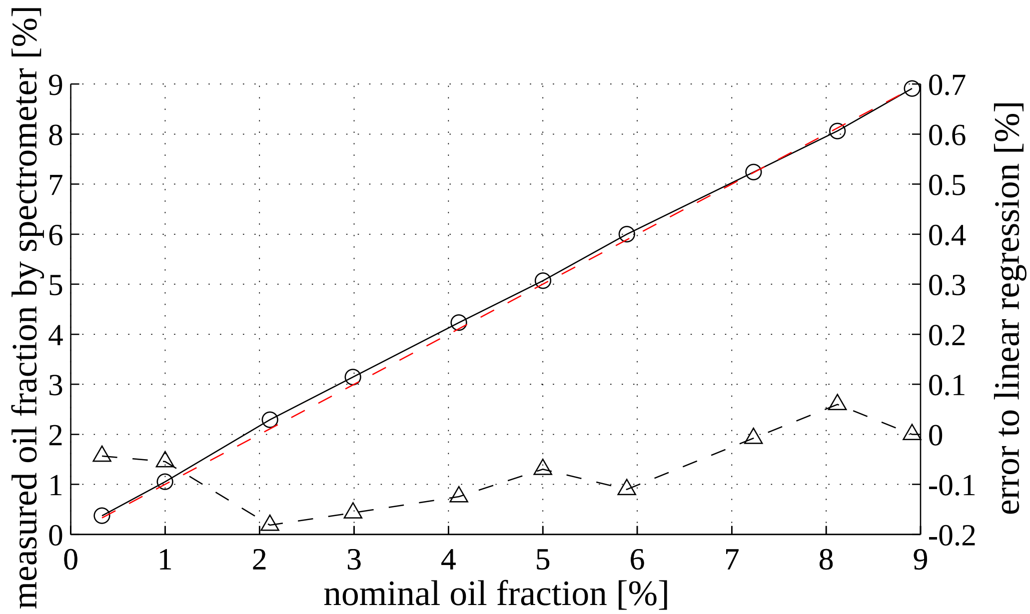

Figure 6.3: *Calibration results (FTIR quant analysis) and error calculation compared to an linear regression. R407C-EAL Arctic 22 CC at p=11.3 bar - 12.6 bar, T=20.8°C,subcooling= 2.3 - 6.3 K*

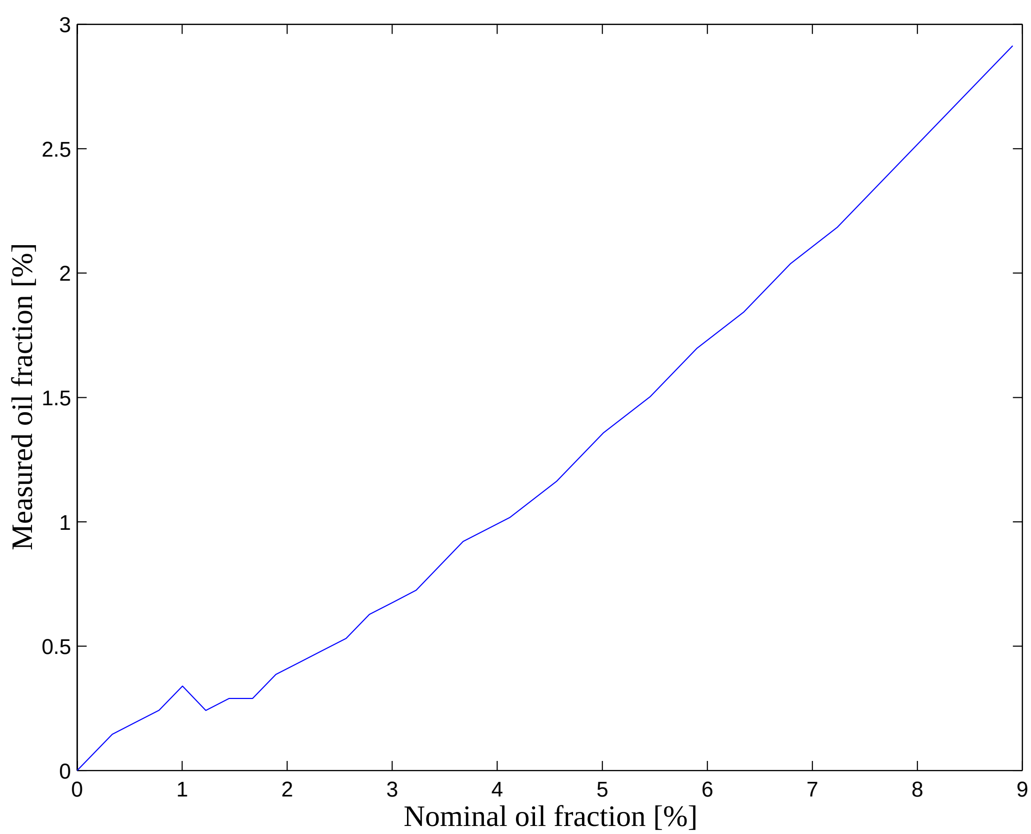

Figure 6.4: *Resulting oil fraction measured with densitymeter. R407C-EAL Arctic 22 CC at p=11.3 bar - 12.6 bar, T=20.8°C,subcooling= 2.3 - 6.3 K*

Bibliography

[1] F. Brand, M. Zehnder, and D. Favrat. **Pompe à chaleur haute température, Phase 1: Solution avec compresseur à injection vapeur**. Final report. Swiss Federal Office of Energy, 2000. ENET-Nr. 9934445.

[2] D. A. C. Compton and D. M. Rayner. **An Analysis of the Vibrational Spectra of C_2F_5I, n-C_3H_7I, and the corresponding Perfluoroalkyl Radicals, $C_2F_5\cdot$ and n-$C_3F_7\cdot$.** *Journal of Physical Chemistry*, 86(9), 1981.

[3] M. O. McLinden, S. A. Klein, E. W. Lemmon, and A.P. Peskin. **Thermodynamic and Transport Properties of Refrigerants and Refrigerant Mixtures - REFPROP Version 6.01**. National Institute of Standards and Technology, 1998.

[4] M. Mizuno and S. Saeki. **Infrared Absorption Intensities of Methylene Fluoride**. *Spectrochemical Acta*, 32A, 1975.

[5] E. Nidegger, D. Reymond, M. Zehnder, and D. Favrat. **Pompe à chaleur bi-étagée à haute performance**. Final report. Swiss Federal Office of Energy, 1997. ENET-Nr. 9400101.

[6] J. Rud Nielsen and C. J. Halley. **Infrared and Raman Spectra of Fluorinated Ethanes**. *Journal of Molecular Spectroscopy*, 17, 1965.

[7] National Institute of Standards and Technology. **Chemistry Webbook**. `http://webbook.nist.gov/chemistry/form-ser.htm`, 2000.

[8] M. Zehnder, D. Favrat, G. Reiner, and C. Brugnoli. **Wärmepumpe mit Hilfskreislauf zur Kondensatunterkühlung, Phase 1**. Final Report. Swiss Federal Office of Energy, 1998. ENET-Nr. 6100005-24.

[9] M. Zehnder, D. Favrat, E. Zahnd, J. Cizmar, G. Reiner, C. Brugnoli, and P. Reis. **Wärmepumpe mit Hilfskreislauf zur Kondensatunterkühlung, Phase 2: Experimentelle Untersuchung**. Final Report. Swiss Federal Office of Energy, 1999. ENET-Nr. 9824787.

[10] Olivier Zürcher. **Contribution to the Heat Transfer Analysis of Natural and Substitute Refrigerants Evaporated in a Smooth Horizontal Tube**. PhD thesis, École Polytechnique Fédérale de Lausanne, 2000.

A. Appendix

A.1 FTIR spectres of the principle components

The following spectral datas were taken at different times and with different spectrometer. Pure R407C was taken with a FTIR Bio-Rad Excalibur spectrometer. The spectres of R134a and the oil spectral data were obtained with the Nicolet Magna-IR 560.

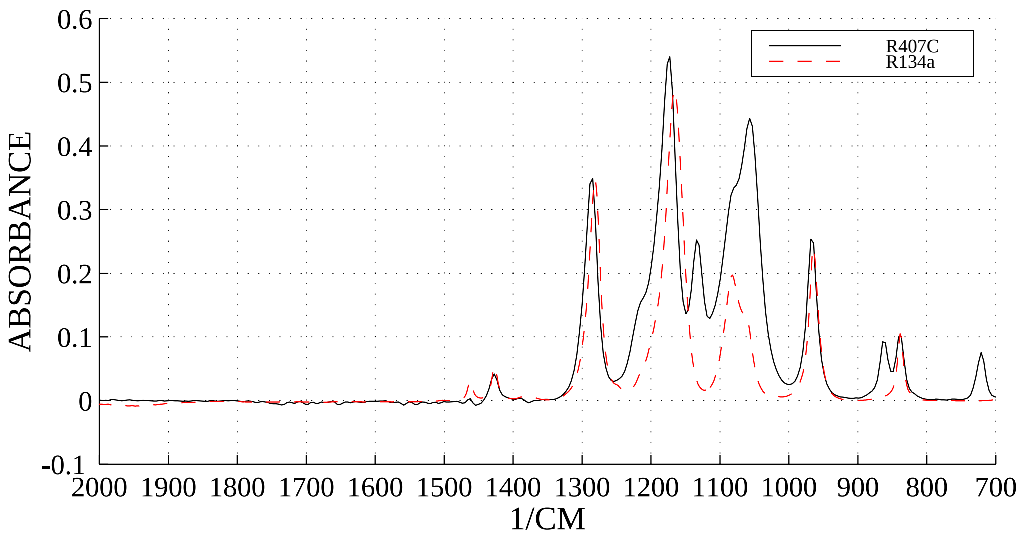

Figure A.1: *Comparison of R407C and R134a FTIR spectres*

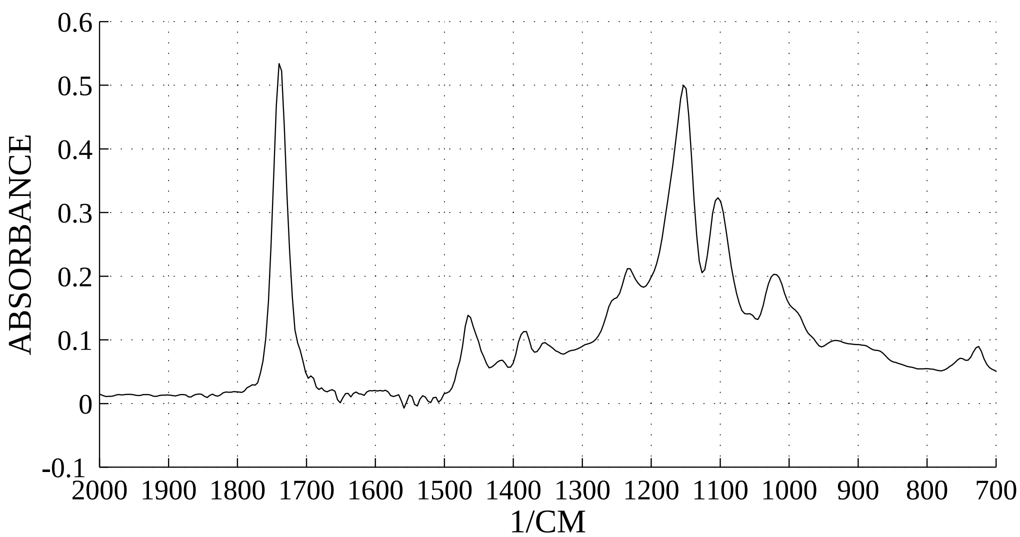

Figure A.2: *Spectral result of pure EAL Arctic 22 CC*

A.2 Calibration of the Radar Emittor VEGAPULS

In the figures A.3 the different measurement are shown. a) Measurement of oil *EAL Arctic 22 CC* in a 40 mm diameter tube with floating plate. Height of the tube 1.2 m. The results show a precision of $< \pm 5$ mm. Weak pressure dependency is seen (about 3 - 6 mm) with the used floating plate.

Comparing calibration tests with water in the same tube, the precision is reached at the same order of magnitude. Given these results this measurement method was not considered for level check in the compressor shafts.

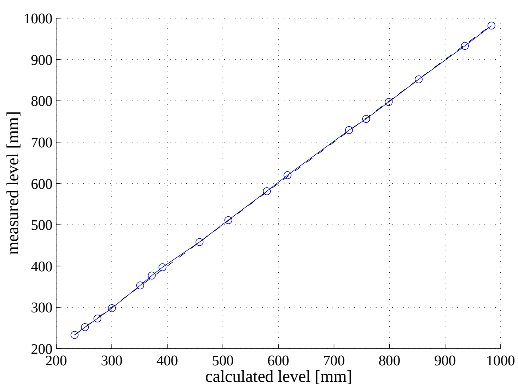

(a) Oil level with floating reflection plate

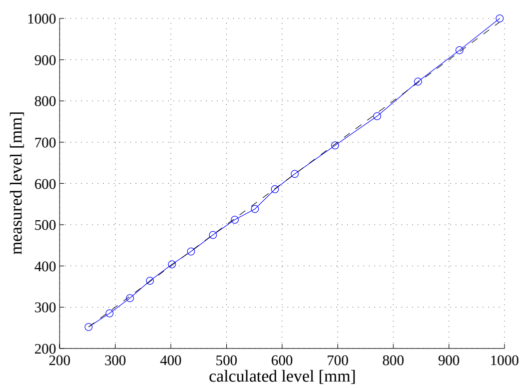

(b) Water level

Figure A.3: *Level measurement by a radar transmitter in a 40 mm tube*

A.3 List of components

PAC-Migroil list of transmittters

D-AQ line:	Cable #	Measurement	Units:	Transmitter
Temperatures:				
200	TR00	free	°C	Thermocouple Type K
201	TR01	T_cp1_in	°C	Thermocouple Type K
202	TR02	T_cp1_out	°C	Thermocouple Type K
203	TR03	T_cp2_in	°C	Thermocouple Type K
204	TR04	T_cp2_out	°C	Thermocouple Type K
205	TR05	T_cd_in	°C	Thermocouple Type K
206	TR06	T_cd_out	°C	Thermocouple Type K
207	TR07	T_eco_liq_out	°C	Thermocouple Type K
208	TR08	T_oh_liq_in	°C	Thermocouple Type K
209	TR09	T_oh_liq_out	°C	Thermocouple Type K
210	TR10	T_oh_vap_out	°C	Thermocouple Type K
211	TR11	T_ev_tube1	°C	Thermocouple Type K
212	TR12	T_ev_tube3	°C	Thermocouple Type K
213	TR13	T_ev_tube5	°C	Thermocouple Type K
214	TR14	T_ev_tube7	°C	Thermocouple Type K
215	TR15	T_ev_tube8	°C	Thermocouple Type K
216	TR16	T_eco_sat_out	°C	Thermocouple Type K
217	TR17	T_eco_sat_in	°C	Thermocouple Type K
Pressures:				
311	PR1	P_cp1_in	bar	Haenni
312	PR2	P_cp1_out	bar	Haenni
313	PR3	P_cp2_in	bar	Haenni
314	PR4	P_cp2_out	bar	Kistler
315	PR5	free	bar	
Power:				
512	E_HP	E_HP_tot	kW	Norma
513	E_cp1	E_cp1	kW	Norma
514	E_cp2	E_cp2	kW	SINEAX PQ502
Mass flow, Density:				
300	FR1	M_flow_1	g/s	Witronic K-20
301	DR1	Dens_1	kg/m3	Witronic K-20
302	FR2	M_flow_2	g/s	Witronic K-100
303	DR2	Dens_2	kg/m3	Witronic K-100
305	DR3	Dens_high_prec	kg/m3	
306	LO1	Level_cp1	mm	
307	LO2	Level_cp2	mm	
Temperatures water:				
600	29	Tw_cd_out_1	°C	Thermocouple Type K
601	22	Tw_cd_out_2	°C	Thermocouple Type K
602	20	Tw_cd_out_3	°C	Thermocouple Type K
603	27	Tw_cd_in_1	°C	Thermocouple Type K
604	26	Tw_cd_in_2	°C	Thermocouple Type K
605	23	Tw_cd_in_3	°C	Thermocouple Type K
Temperatures air, fins:				
606	11	Tair_ev_out_1	°C	Thermocouple Type K
607	85	Tair_ev_out_2	°C	Thermocouple Type K
608	86	Tair_ev_out_3	°C	Thermocouple Type K
609	87	Tair_ev_in_1	°C	Thermocouple Type K
610	88	Tair_ev_in_2	°C	Thermocouple Type K
611	1	Tair_ev_in_3	°C	Thermocouple Type K
614		Tsurf_fin_in	°C	Thermocouple Type K
615		Tsurf_fin_out	°C	Thermocouple Type K
619	81	Tigloo	°C	Thermocouple Type K
Pressure drops:				
500	DP1	dp_evap	mbar	Furness
501	DP2	dp_air_flow	mbar	Furness
Humidity:				
507	HR	hum_rel_air	%	Rotronic Hygromer
508	TA_hr	T_air_hum_rel	°C	Rotronic Hygromer

A.4 List of measurement points

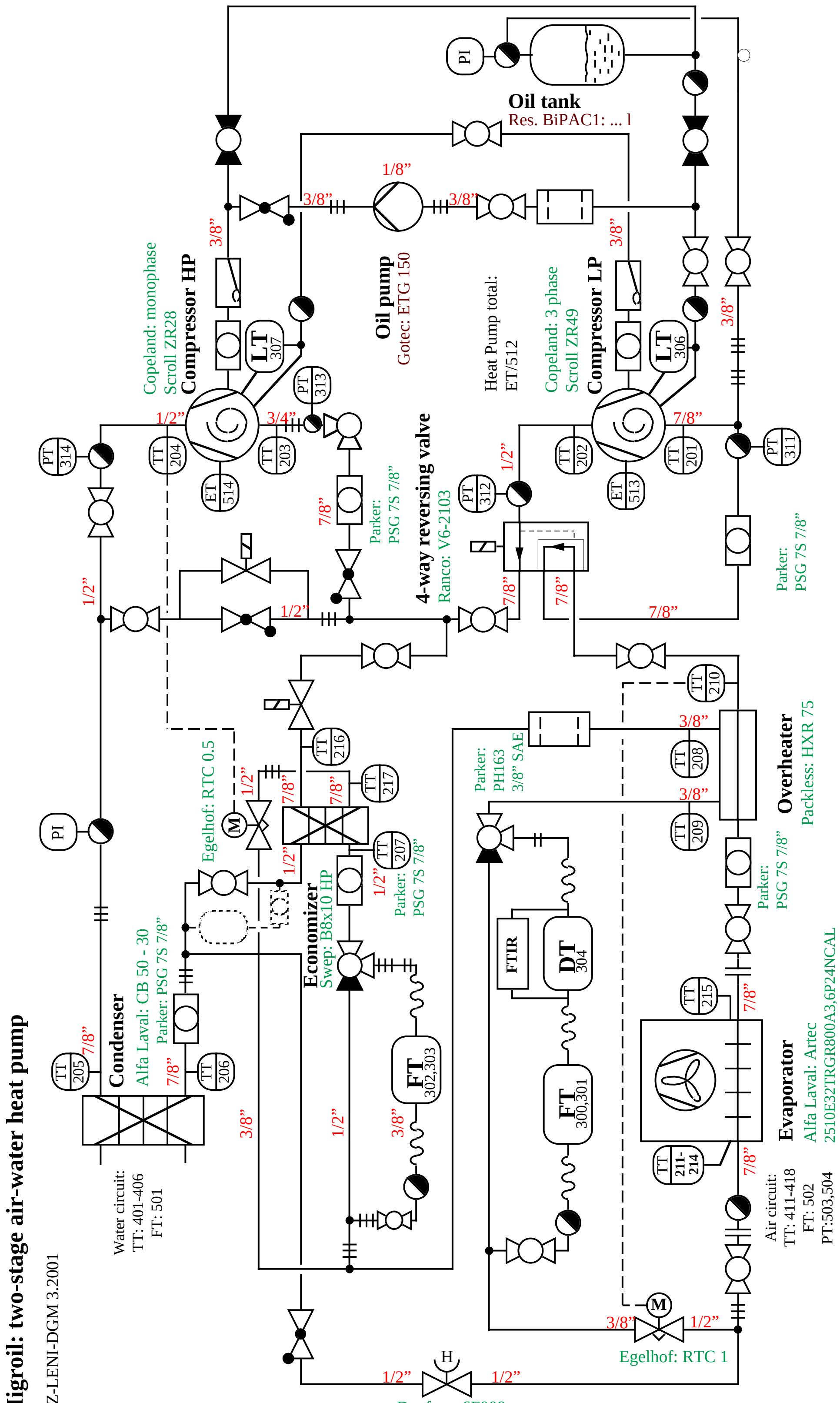

Figure A.4: *Schema with components and measurement locations*

Liste de capteurs PAC-Migroil

No borne:	No Câble	lieu mesure	Sonde	Fct. d'étalonnage	Signature	Date
Température						
101	TR1	cp_bp_in				
102	TR2	cp_bp_out				
103	TR3	cp_hp_in				
104	TR4	cp_hp_out				
105	TR5	cd_in				
106	TR6	cd_out				
107	TR7	eco_liq_out				
108	TR8	sg_oh_liq_in				
109	TR9	sg_oh_liq_out				
110	TR10	ev_in				
111	TR11	ev_out				
112	TR12	sg_oh_vap_out				
113	TR13	eco_biph_in				
114	TR14	eco_biph_out				
Pression, Puissances						
201	PR1	cp_bp_in				
202	PR2	cp_bp_out				
203	PR3	cp_hp_in				
204	PR4	cp_hp_out				
205	PR5	ev_in				
211	E1	cp_bp				
212	E2	cp_hp				
Débit, Densité, Niv liquide						
301	FR1	sg_oh_liq_out				
302	DR1	sg_oh_liq_out				
303	FR2	eco_liq_out				
304	DR2	eco_liq_out				
305	DR3	sg_oh_liq_out				
306	LO1	cp_bp_in				
307	LO2	cp_hp_in				
Température						
401	TE1	eau_cd_in_1				
402	TE2	eau_cd_in_2				
403	TE3	eau_cd_in_3				
404	TE4	eau_cd_out_1				
405	TE5	eau_cd_out_2				
406	TE6	eau_cd_out_3				
411	TA1	air_ev_in_1				
412	TA2	air_ev_in_2				
413	TA3	air_ev_in_3				
414	TA4	air_ev_out_1				
415	TA5	air_ev_out_2				
416	TA6	air_ev_out_3				
417	TA7	air_ail_in				
418	TA8	air_ail_out				
Débits, Pressions différentielles+A15						
501	FE1	eau_cd_in				
502	FA1	air_ev_out				
503	DP1	dp_evap				
504	DP2	dp_pac				